Molecular Alignment of Homoleptic Iridium Phosphors in Organic Light-Emitting Diodes.

Moon Chul Jung[1], John Facendola[2], Jongchan Kim[3], Daniel Sylvinson Muthiah Ravinson[2], Peter I. Djurovich[2], Stephen R. Forrest[3,4], Mark E. Thompson[1,2]*

1. Mork Family Department of Chemical Engineering and Materials Science, University of Southern California, Los Angeles, California 90089, United States

2. Department of Chemistry, University of Southern California, Los Angeles, California 90089, United States

3. Department of Electrical and Computer Engineering, University of Michigan, Ann Arbor, Michigan 48109, United States

4. Department of Physics and Materials Science and Engineering, University of Michigan, Ann Arbor, Michigan 48109, United States

Email: met@usc.edu

ToC Graphic and Caption:

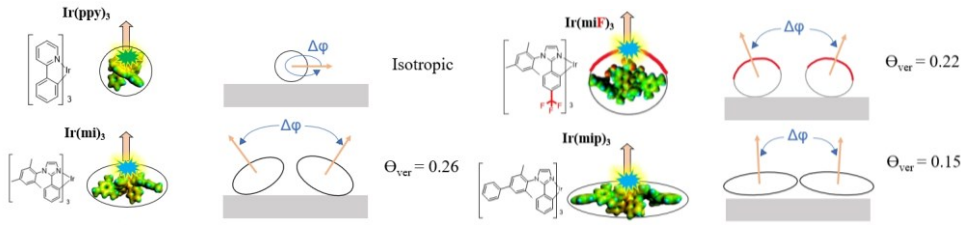

Dopant alignment in doped, vacuum deposited films can be promoted by molecular asymmetry and/or asymmetry in the dopant's electrostatic surface potential.

This is the author manuscript accepted for publication and has undergone full peer review but has not been through the copyediting, typesetting, pagination and proofreading process, which may lead to differences between this version and the Version of Record. Please cite this article as doi: 10.1002/adma.202102882.

Abstract

The orientation of facial (*fac*) *tris*-cyclometalated iridium complexes in doped films prepared by vacuum deposition is investigated by altering the physical shape and electronic asymmetry in the molecular structure. Angle-dependent photoluminescence spectroscopy and Fourier-plane imaging microscopy show that the orientation of roughly spherical *fac*-tris(2-phenylpyridyl)iridium ($Ir(ppy)_3$) is isotropic, whereas complexes that are oblate spheroids, *fac*-tris(mesityl-2-phenyl-1H-imidazole)iridium ($Ir(mi)_3$) and *fac*-tris((3,5-dimethyl-[1,1'-biphenyl]-4-yl)-2-phenyl-1H-imidazole)iridium ($Ir(mip)_3$), have a net horizontal alignment of their transition dipole moments. Optical anisotropy factors of 0.26 and 0.15, respectively, are obtained from the latter complexes when doped into *tris*(4-(9H-carbazol-9-yl)phenyl)amine host thin films. The horizontal alignment is attributed to the favorable van der Waals interaction between the oblate Ir complexes and host material. Trifluoromethyl groups substituted on one polar face of the $Ir(ppy)_3$ and $Ir(mi)_3$ complexes introduce chemical asymmetries in the molecules at the expense of their oblate shapes. The anisotropy factors of films doped with these substituted derivatives are lower relative to the parent complexes, indicating that the fluorinated patches reinforce horizontal alignment during deposition. High efficiencies obtained from organic light emitting diodes prepared using the Ir dopants is attributed, in part, to improved outcoupling of electroluminescence brought about by molecular alignment.

Introduction

Organic light emitting diodes (OLEDs) have been intensively investigated due to their capacity to give high luminance efficiency and color quality.[1] Even though 100% internal quantum efficiency has been achieved using phosphorescent dopants, fabrication of extremely high efficiency OLEDs has been hampered by relatively inefficient light extraction from the device.[2, 3] Typically, 80% of photons produced by the OLED are lost due to waveguiding, absorption and coupling to surface plasmon modes.[2, 4] Several extrinsic approaches have been introduced to reduce waveguiding and absorption losses,[5] including the use of microlens arrays,[6, 7] scattering particles[8] and mechanical roughening of the substrate.[9] By using a combination of these approaches, the losses of the light generated by electroluminescence drop to *ca.* 30%.[7] The outcoupling can be further improved by controlling alignment of transition dipole moments (TDMs) of the emitting molecules in emissive layer. Considering that light is primarily emitted perpendicular to the TDM, alignment of the TDM parallel to the substrate can reduce the excitation of waveguide, surface plasmon and lossy metal modes, while increasing the air and substrate modes.[10, 11-13] The degree of alignment of the TDM is given by the anisotropy factor, Θ, which corresponds to the ratio of the emitted power of the projection of the net TDM onto the axis perpendicular to the substrate (p_z^2), to the sum of the total power of the light emitted: $\left[\Theta = {p_z^2}\Big/{\left(p_x^2 + p_y^2 + p_z^2\right)}\right]$. Thus, a complex with an isotropic TDM orientation gives Θ = 0.33, whereas one with all TDMs parallel to the substrate (in the $x - y$ plane) gives Θ = 0.[14] *Bis*-cyclometalated Ir diketonate complexes are common emissive dopants in OLEDs that show anisotropy factors of 0.22-0.25 in vacuum deposited films, indicating a net in-plane TDM alignment.[15, 16] In contrast, several homoleptic *tris*-cyclometalated Ir complexes such as $Ir(ppy)_3$, are isotropic in doped films (Θ = 0.33).[12, 16, 17]

Molecular alignment in vacuum deposited films requires that diffusion along the surface be sufficiently rapid for molecules to find a preferred orientation before being overcoated with additional deposited material.[18] However, the underlying molecular features needed to guide the alignment of emissive dopants in the films is not yet completely understood. For complexes such as rigid-rod emitters, association of the molecule with the organic surface on deposition drives a horizontal arrangement.[3, 12, 19] For square-planar platinum-based emitters, horizontal alignment can be induced by the orientation of the host[20] or by introducing a flat, ordered templating layer before depositing the film.[21] For octahedral $(C^N)_2Ir(L^X)$ type complexes, Jurow *et al.*, proposed that the organic/vacuum interface induces reorientation of dopants due to the inherent chemical asymmetries of the surface. Here, C^N represents a cyclometalated ligand and L^X an auxiliary ligand.[22] Recently it has been shown that molecular alignment in a series of homoleptic Ir complexes can be correlated to the effects of geometric anisotropy and electrostatic interactions with the surface of a growing film.[13, 23] Thus, it should be possible to design features into a homoleptic Ir complex that favor a specific molecular orientation capable of enhancing the horizontal alignment of the TDM that improves outcoupling of the emitted light.

In 2014, Udagawa, *et al.,* reported a blue-emitting OLED with an external quantum efficiency of EQE = 30% that utilized tris(mesityl-2-phenyl-1H-imidazole)iridium [$Ir(mi)_3$, **Figure 1**].[24] The high EQE in these OLEDs suggests that the TDMs of the $Ir(mi)_3$ dopants are horizontally (in-plane) aligned. Here we use angle dependent-photoluminescence spectroscopy (ADPS)[14, 25] and Fourier-plane imaging microscopy (FPIM)[26] to measure the alignment of the TDMs of $Ir(mi)_3$, $Ir(ppy)_3$ and several substituted derivatives of these complexes (Figure 1). A net horizontal alignment of TDMs is observed for all complexes, aside from $Ir(ppy)_3$, leading to OLEDs with EQEs = 22.3-30.5%. In this family of emitters, both its molecular shape (*i.e.*, deviation from roughly spheroidal) and non-uniformity in the electrostatic surface potential (ESP) of an emitter gives rise to a preferred dopant alignment. The non-uniformity in the ESP markedly increases upon addition of electron withdrawing groups to the aryl groups of the cyclometalating ligands in the organometallic complexes,[23] and is found to enhance alignment of the dopants. Complexes with highly non-uniform ESP will hereafter be referred to as having high “chemical asymmetry”.

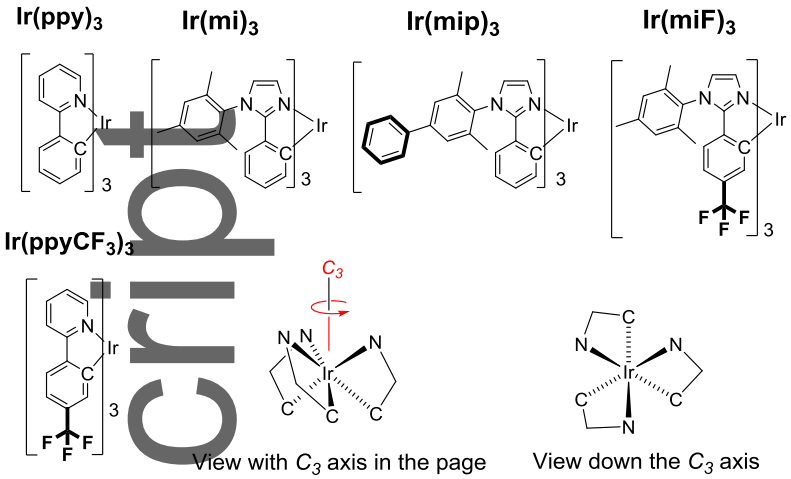

Figure 1. The five *fac*-Ir(C^N)$_3$ complexes studied here. The three C^N ligands are equivalent in these facial complexes. Illustrations of the three-dimensional structures of these complexes are shown with the C_3 axis lying within and perpendicular to the plane of page.

Results and discussion

Characterization of the complexes

The Ir complexes were synthesized using modified versions of literature methods[27, 28] and characterization data for the compounds are provided in the supporting information. All the complexes were obtained as facial (*fac*) isomers. Emission spectra of the phenylimidazole-based compounds display sky blue luminescence, with Ir(miF)$_3$ showing a slight bathochromic shift relative to the other two derivatives (**Figure 2**). The Ir(ppy)$_3$ and Ir(ppyCF$_3$)$_3$ complexes emit in the green, with the CF_3 substituents leading to a small blue shift in emission. The complexes have photoluminescence lifetimes (τ) in the microsecond range at both room temperature and 77K, and high quantum yields (Φ_{PL} > 90%) (see Tables 1, S1 and S2 for the full photophysical characterization of the compounds). The values for τ and Φ_{PL} observed are comparable to those found in other homoleptic *tris*-cyclometalated iridium (III) complexes.[28, 29] The energies for the highest occupied (HOMO) and lowest unoccupied molecular orbital (LUMO) were determined using solution electrochemical measurements (Table 1). The presence of the electron withdrawing trifluoromethyl groups in Ir(miF)$_3$ and Ir(ppyCF$_3$)$_3$ stabilize the HOMO energies by 0.30 eV relative to their parent complexes. The permanent dipole moments (PDM) of the complexes were calculated using density functional theory (DFT) and given in Table 1 and shown in Figure S18. All of the compounds have their PDM directed along the C_3 axis, with the CF_3 substitution leading to a substantial increase in the magnitude of the PDM.

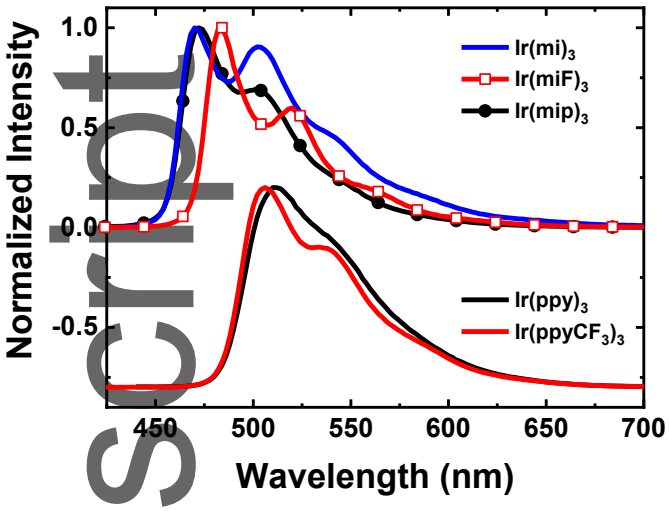

Figure 2. Emission spectra and photophysical parameters for the *fac*-Ir(C^N)$_3$ complexes in 2-methyltetrahydrofuran (2-MeTHF) at room temperature.

Here we compare the spatial anisotropies of the five emissive dopants, with shapes ranging from roughly spherical to oblate spheroidal. Space-filling models of the complexes with views looking both along and down the C_3 axis are shown in **Figure 3**. To quantify the anisotropy, the 3D moment of inertia matrix of each complex was computed and diagonalized to yield three eigenvalues corresponding to the dimensions along its three principal axes of an ellipsoid that encloses the molecule (see Supporting Information for calculation details). The aspect ratio of the molecule is defined as the ratio of the eigenvalues for the major and minor axes. The Ir(ppy)$_3$ complex has a slightly ellipsoidal shape (aspect ratio of 1.2) due to a compression along the C_3 axis. The Ir(mi)$_3$ complex has a more oblate spheroidal shape, with an aspect ratio of 2.2. Extending the imidazolyl ligand by appending an additional phenyl group in Ir(mip)$_3$ increases the aspect ratio to 3.0. Addition of CF_3 groups decreases the aspect ratio relative to the parent complexes, giving ratios for Ir(miF)$_3$ of 1.9, and Ir(ppyCF$_3$)$_3$ of 1.0. In all cases, the long axis of the oblate shape lies perpendicular to the C_3 axis.

The molecular orientation of the luminescent complex relative to the substrate can be established from the optical anisotropy of dopant-based films (*vide infra*). However, to do so the dopant's TDM needs to be mapped onto the molecular frame of the compound. This mapping of the TDM of the triplet excited state for each dopant was carried out using time-dependent density functional theory (TDDFT) with the zero-order regular approximation (ZORA) that incorporates spin-orbit coupling.[30] The TDM is localized in the plane of a single Ir(C^N) moiety with the origin on the Ir atom (**Figure 4**). The C_3 axis of the Ir(C^N)$_3$ complex leads to three such TDMs in the molecule whose orientations lie at the angle, δ, relative to the Ir-N bond. Mapping the orientation of the TDM onto the full molecular frame gives its angle, α, with the C_3 axis. The Ir(C^N)$_3$ complexes considered here have TDMs that are nearly orthogonal to the C_3 axis (α = 84-94°). Thus, a horizontal TDM alignment is indicative a dopant oriented with the C_3 axis perpendicular to the substrate. One might speculate that slight deviation from perfect angle (α = 90°) might induce a meaningful change in anisotropy value.

However, based on a mathematical representation that relates the value of Θ to the angle δ for a facial octahedral complex and relation between δ and α,[22] Θ changes no more than 0.01 for a decrease in α from 90° to 84°. This is within the error range of APDS measurement (0.01-0.04), indicating directions of TDMs in all compounds are close to be in ideal condition.

Table 1. Maximum emission wavelength (λ_{max}), photoluminescence efficiency (Φ_{PL}), lifetime (τ), HOMO/LUMO and magnitude of permanent dipole moment of the *fac*-Ir(C^N)$_3$ complexes.

	λ_{max} (nm)[a]	Φ_{PL}[a]	τ (μs)[a]	HOMO/LUMO (eV)[b]	Permanent dipole moment (Debye)[c]
Ir(mi)$_3$	464	0.91	2.0	-4.9/[d]	6.9
Ir(mip)$_3$	466	0.98	1.8	-4.9/-1.5	6.7
Ir(miF)$_3$	484	0.99	2.5	-5.2/-1.5	12.7
Ir(ppy)$_3$	512	1.0	1.2	-5.2/-1.7	6.4
Ir(ppyCF$_3$)$_3$	506	0.98	1.2	-5.5/-1.9	16.3

[a] Measured in 2-MeTHF solution. [b] HOMO and LUMO were determined using the electrochemical potentials as reported in reference [31]. [c] Calculated using DFT (B3LYP/LACV3P**). [d] The reduction potential for Ir(mi)$_3$ was not observable in dimethylformamide (DMF) solvent.

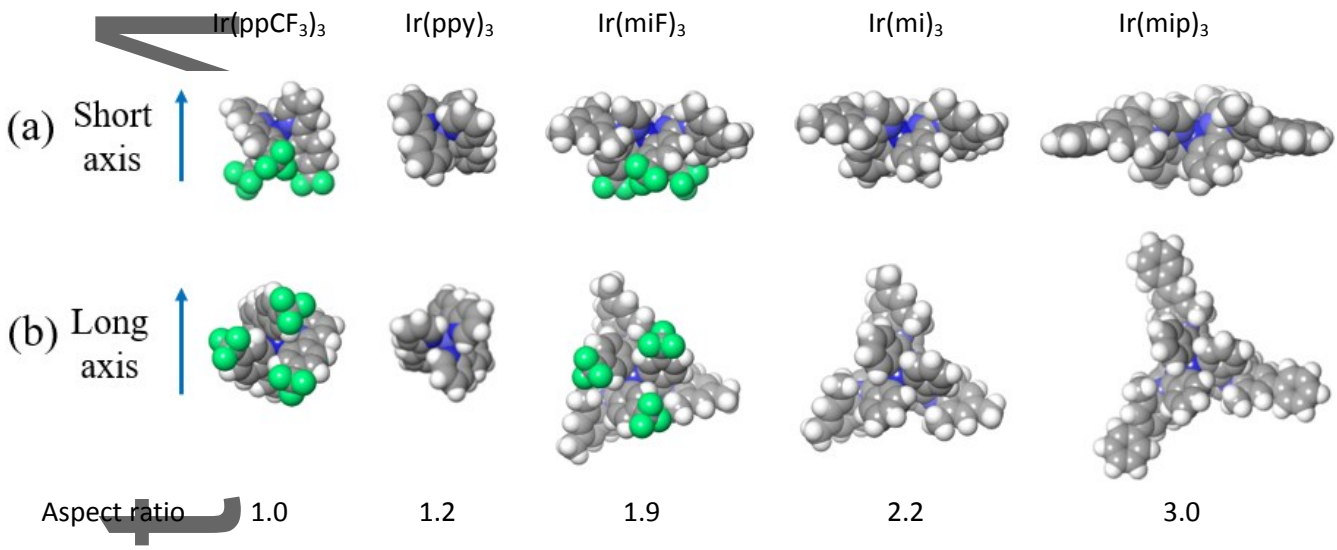

Figure 3. Space-filling models of each *fac*-Ir(C^N)$_3$ complex with side (a) and top (b) views to illustrate structural differences.

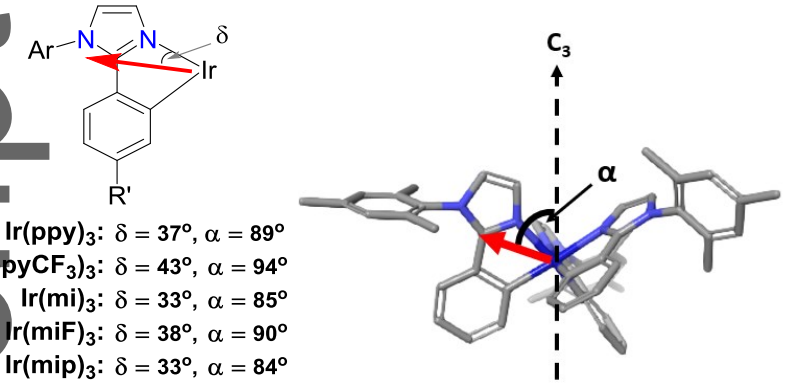

Figure 4. The TDM (red arrow) of the *fac*-Ir(C^N)$_3$ complexes is in the Ir(C^N) plane, subtending an angle δ between the TDM and the Ir-N bond. The C_3 axis gives three equivalent TDMs, with the angle α between the TDMs and the C_3.

The role of structure in dopant alignment

The three phenyl-imidazole complexes were investigated using ADPS (see SI for details) in vacuum deposited films doped at 10 wt% in *tris*(4-carbazoyl-9-ylphenyl)amine (TCTA) or 3,3-di(9H-carbazol-9-yl)-1,1-biphenyl (mCBP) hosts (Figures S20 and S21). Anisotropy factors measured for these films are insensitive to the host (see **Table 2**).[32] Values obtained for films doped with Ir(mi)$_3$ (Θ = 0.26) are similar to those reported for heteroleptic iridium complexes, and are consistent with the high EQE observed for Ir(mi)$_3$ based OLEDs reported by Udagawa, *et al.*[24] Molecular alignment in heteroleptic iridium complexes (*i.e.* (ppy)$_2$Ir(acac)) is thought to be driven by the chemical asymmetry induced by the auxiliary ligand;[11, 17, 32-34] however, this rationale is problematic for explaining alignment of the homoleptic Ir(mi)$_3$ complex. We postulate instead that the oblate shape of the molecule favors van der Waals π-π interactions between the dopant and the organic surface when the long axis of the ellipsoid is parallel to the surface (C_3 axis perpendicular).[35] Similar π-π interactions have been used to account for the alignment of planar[21] and rigid rod-like[19, 32] dopants in vacuum deposited films. This explanation predicts that the spherical shape of Ir(ppy)$_3$ would not favor a particular TDM orientation, consistent with the optical isotropy in doped thin films.[33, 34]

Table 2. Optical anisotropy factors of iridium complexes.

Emitter	Host	Θ
$(ppy)_2Ir(acac)$	CBP	0.23[17]
$Ir(ppy)_3$	TCTA:B3PYMPM	0.33[33]
	CBP	0.32[36]
	TCTA:26DCzPPy	0.35
$Ir(ppyCF_3)_3$	TCTA:26DCzPPy	0.29
$Ir(mi)_3$	TCTA	0.26
	mCBP	0.25
$Ir(miF)_3$	TCTA	0.22
	mCBP	0.22
$Ir(mip)_3$	TCTA	0.15
	mCBP	0.16

The anisotropy data for $Ir(mip)_3$ doped films supports the hypothesis that maximizing the π-π interaction area of the dopant and organic surface, and thus the van der Waals attractive forces, drives horizontal alignment. The value found for $Ir(mip)_3$ (Θ = 0.15) is one of the lowest among Ir complexes.[11, 13, 17, 32-34] Molecular interactions between $Ir(mip)_3$ and the host during deposition is expected to be strongest when the long axis of the oblate spheroid is parallel to the substrate. With this in mind we also prepared a larger analog of $Ir(mip)_3$ by replacing the para-methyl group on each mip ligand with a phenyl ring, thus further increasing the aspect ratio to 3.7 (see $Ir(mipp)_3$ in Scheme S1). Unfortunately, $Ir(mipp)_3$ decomposed upon sublimation precluding the study of vacuum deposited films using this derivative.

A similar correlation between alignment to the substrate plane and dopant shape has been reported for a series of cyano-substituted phenyl-imidazole iridium compounds by Kim, *et al.* (Scheme 1).[13] Aspect ratios for these complexes calculated as described above give values ranging from 1.4 to 2.9 (see Table S3). The values of Θ for these dopants were also found to decrease with an increase in the aspect ratio of the dopant. The authors modelled the dopant alignment using a combination of Coulomb and van der Waals forces between the host and the dopants. In their model, the Coulomb force exerted by the permanent dipole moment is roughly equal when the PDM is pointed either at or away from the substrate. Since their modeling predicted a significantly lower magnitude for Coulomb relative to the van der Waals interactions, the Coulomb term only becomes relevant for dopants having a small aspect ratio, especially when deposited in host materials with high PDMs (the host molecules used in the Kim study has a PDM of 5.0 D, Table S4).[13, 15] The energetic models by Kim, *et al.,* thus suggest that Coulomb forces acting on molecules with high dipole moments should favor dopant alignment. Countering this proposal is the fact that *fac*-$Ir(ppy)_3$ has a PDM of 6.4 D, and is isotropic in host materials of varying polarity.[36] In contrast, a model by Jurow, *et al.,*[22] that incorporates the effects of chemical asymmetry can also be used to explain the net alignment of dopants of Kim *et al*. with low aspect ratios since these tris-chelated phenyl-imidazolyl complexes have nitrile groups situated close together on the molecular surface.

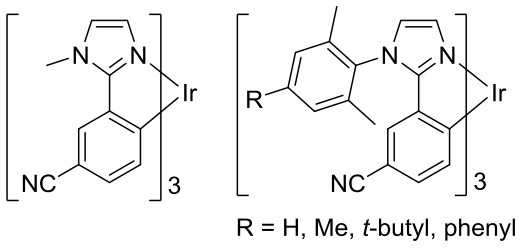

Scheme 1: Ir dopants used in Kim, *et al.*

<u>The role of chemical asymmetry in dopant alignment</u>

We also investigated the impact of chemical asymmetry in the iridium phenyl-imidazole complexes by examining a derivative with trifluoromethyl substituents. The CF_3 groups in $Ir(miF)_3$ significantly alter the chemical asymmetry of the complex by presenting a fluorinated region on one face of the molecule (Figure 3), which increases the PDM from 6.9 D for $Ir(mi)_3$ to 12.7 D for $Ir(miF)_3$. While the larger PDM increases Coulomb attraction between host and dopant, the dipole moments of the host materials chosen for our study are low (PDM = 0.1-2.9 D, Table S4). The CF_3 groups decrease the aspect ratio of $Ir(miF)_3$ to 1.9, which is expected to decrease the degree of horizontal alignment. Nevertheless, the anisotropy factor measured for $Ir(miF)_3$ is lower than that of $Ir(mi)_3$ (Θ = 0.22 $\pm$ 0.02 and 0.26 $\pm$ 0.02, respectively). Moreover, the anisotropy factors for $Ir(miF)_3$ are unaffected by the magnitude of the dipole moment of the host matrix. Apparently, the electronic asymmetry imparted by the CF_3 groups compensates for loss in alignment due to the lower aspect ratio of $Ir(miF)_3$. Molecular interactions between the trifluoromethyl moieties and the aromatic π-systems of the host are disfavored,[37] thus it is expected that the dopants will orient with their fluorine-rich side directed away from the substrate toward the vacuum during deposition. Consequently, horizontal orientation of the $Ir(miF)_3$ complex is promoted by CF_3 groups even though attractive interactions between the π-system of the host and the dopant are diminished by the substituents.

To further demonstrate the contribution of chemical asymmetry to the molecular orientation, trifluoromethyl groups were introduced onto the ligands of $Ir(ppy)_3$ to make $Ir(ppyCF_3)_3$ (Figure 1).

FPIM measurements (see SI for details) were conducted on vapor deposited films consisting of 10% of $Ir(ppy)_3$ or $Ir(ppyCF_3)_3$ doped (TCTA) : 2,6-bis[3-(9H-carbazol-9-yl)phenyl]pyridine (26DCzPPY) mixed host materials to determine the orientation of the TDMs (Figure S22).[26] The anisotropy factor found for $Ir(ppyCF_3)_3$ is smaller than that of $Ir(ppy)_3$ (Θ = 0.29 and 0.35, respectively) despite the relatively spherical shape of $Ir(ppyCF_3)_3$ (aspect ratio = 1.0). Thus, the net horizontal alignment of $Ir(ppyCF_3)_3$ compared to $Ir(ppy)_3$ is attributed to the CF_3 groups, suggesting that chemical asymmetry can increase the degree of horizontal alignment of the TDMs in the thin film.

A plot of the anisotropy factor versus the aspect ratio of the compounds studied here, as well as the cyano-substituted derivatives of Kim, *et al.,* is shown in **Figure 5a**. The compounds are clustered into three groups depending the type (or absence) of substituent, with each grouping having a similar dependence of Θ on the aspect ratio. The presence of chemical asymmetry can be illustrated using the electrostatic surface potential of the complex. The ESP calculated for the unsubstituted complexes is relatively uniform, whereas in both the CF_3- and cyano-substituted derivatives, the ESPs are non-uniform (**Figure 5b**). The color of the ESP surface is based on the energy of a proton moved across the surface. A large negative energy (red) denotes a high negative charge at the surface, whereas a large positive energy (blue) indicates a high positive charge at the surface of the molecule. The most negative ESPs of the acceptor substituted molecules are symmetrically disposed around the C_3 axis, forming a "patch" of high ESP. The patch of high ESP reinforces an alignment of the molecule that favors low Θ. Dopant alignment appears to be a cooperative process, with both high aspect ratio and non-uniform ESP contributing to a lower Θ. Interestingly, the cyano substituents promote a higher degree of dopant alignment than CF_3-substitution for a given dopant aspect ratio. One possible explanation to account for this effect is a difference in the electrostatic force exerted by the various substituents. The partial charge calculated for the cyano-nitrogens of D3 is -0.53 versus -0.27 for the fluorine atoms in $Ir(miF)_3$. The larger magnitude of charge on the cyano group results in an increased electrostatic force on the face of the molecule than one generated by the trifluoromethyl groups, thereby promoting more effective alignment in the former dopant. Note that D3 and $Ir(miF)_3$ have their substituents on different positions of the phenyl-imidazole ligand; D3 is *para* whereas the CF_3 in $Ir(miF)_3$ is *meta* to Ir. However, when $Ir(miF)_3$ is modelled with the CF_3 groups *para* to Ir the partial charge at the fluorine atoms is -0.22, close to that of $Ir(miF)_3$. The magnitude of electrostatic charge on the surface of the molecule depends more on the identity of the functional group than its substitution site.

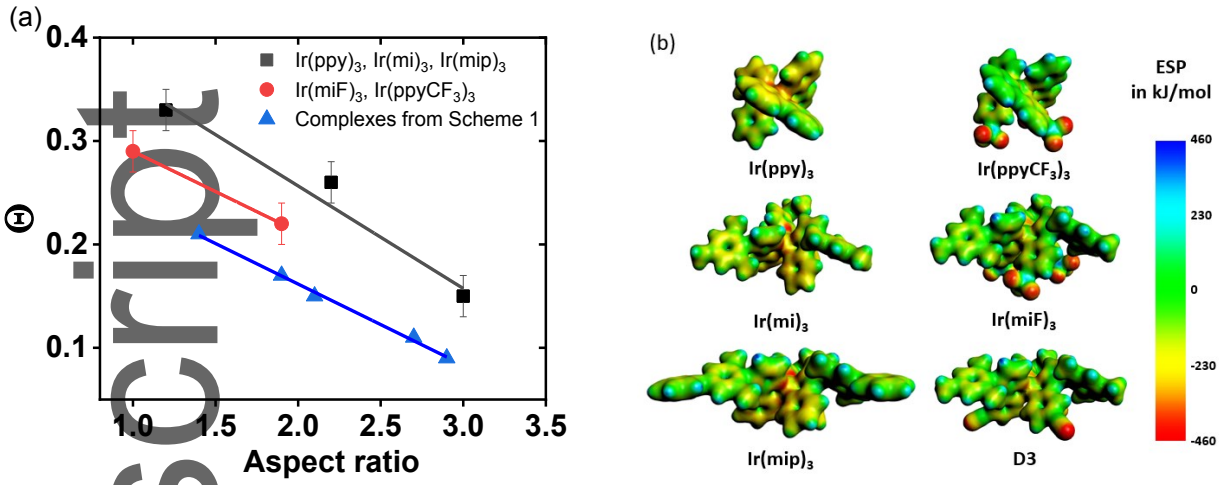

Figure 5. (a) Anisotropy values as a function of aspect ratio for molecules studied here and the cyano-substituted complexes from reference [13] (Scheme 1). (b) Electrostatic surface potential plots for Ir(C^N)$_3$. D3 is the complex in **Scheme 1** with R = CH_3, the closest analog of Ir(mi)$_3$ and Ir(miF)$_3$.

Electroluminescence of aligned emitter molecules

OLEDs utilizing the five Ir(C^N)$_3$ compounds investigated here as emissive dopants illustrate how their enhanced horizontal TDM alignment affects outcoupling, and in turn external quantum efficiency. **Figure 6** illustrates the device along with the performance data obtained using the structure: glass substrate / 70 nm ITO / 50 nm 4,4'-cyclohexylidenebis [N,N-bis(4-methylphenyl)benzenamine] (TAPC) / 15 nm EML / 50 nm 3,3',5,5'-tetra[(*m*-pyridyl)-phen-3-yl]biphenyl (BP4mPy) / 1.5 nm 8-hydroxyquinolinato lithium (LiQ) / 100 nm Al. The emissive layers (EML) comprise the iridium complexes doped at 10 vol% into a TCTA-26DCzPPY mixed host (ratio = 2:1). The mixed host system was employed to enhance injection and transport of charges in the emissive layer, resulting in improved charge balance in the EML and low drive voltage.[38] The device performance parameters are summarized in **Table 3**.

Table 3. Summary of device performance with simulated EQE and outcoupling efficiency

	V_T [a)]	Experimental EQE_{max}	Φ_{PL} [b)]	Outcoupling efficiency	Simulated EQE	CIE
$Ir(ppy)_3$	2.9 V	22.3 %	0.91	0.246	22.4 %	(0.26, 0.63)
$Ir(ppyCF_3)_3$	4.5 V	20.0 %	0.82	0.254	20.8 %	(0.26, 0.63)
$Ir(mi)_3$	2.5 V	26.4 %	0.94	0.286	26.9 %	(0.23, 0.53)
$Ir(miF)_3$	3.9 V	25.5 %	0.91	0.302	27.5 %	(0.22, 0.53)
$Ir(mip)_3$	2.8 V	30.5 %	0.97	0.328	31.8 %	(0.25, 0.58)

[a)]Turn-on voltage is defined as the voltage at brightness 0.1 cd m^{-2}, [b)] Photoluminescence quantum yield measured for the dopant in a TCTA:26DCzPPy mixed film.

As shown in **Figure 6b**, the electroluminescence (EL) spectra have distinct vibronic features and no detectable host emission, consistent with efficient exciton trapping on the dopant. The maximum efficiency of the device using $Ir(ppy)_3$ (EQE = 22.3±0.6%) is close to the maximum expected value for an isotropic dopant and no extrinsic outcoupling enhancements from a glass substrate,[12] whereas the efficiency of devices using $Ir(mi)_3$, $Ir(miF)_3$ and $Ir(mip)_3$ (EQE = 26.4±0.4, 25.5±0.2 and 30.5±0.6 % respectively) due to their horizontal TDM alignment. Note that OLEDs using dopants with CF_3 substituents, despite having low values for Θ in films, are less efficient than the analogous devices using the parent dopants, likely due to their low photoluminescence quantum yields.

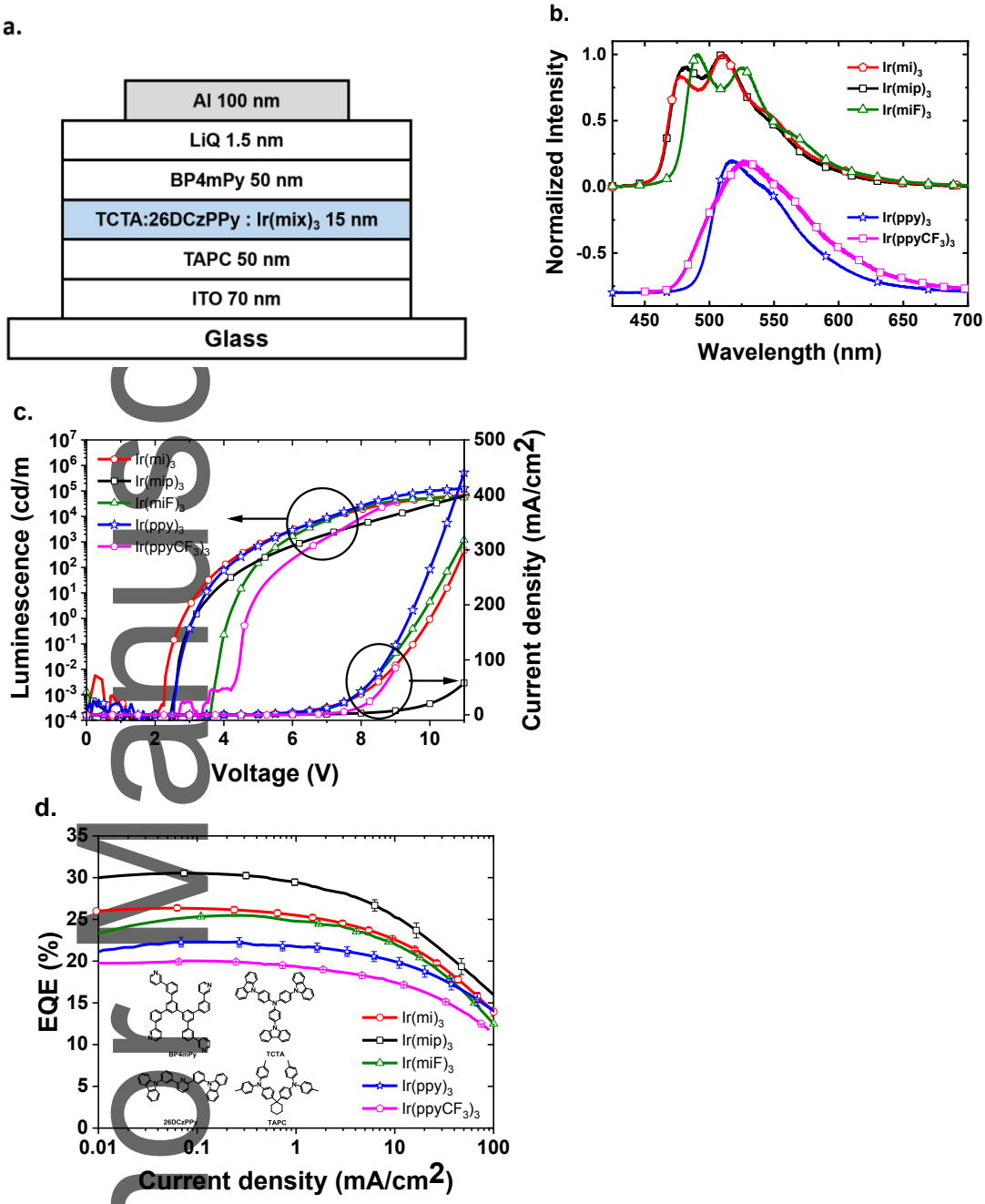

Figure 6. a.) Device architecture for all OLEDs. TCTA and 26DCzPPy are mixed with 2:1 ratio in the emissive layer with 10 vol% doping concentration, b.) Electroluminescence spectra of $Ir(mi)_3$ (red), $Ir(mip)_3$ (black), $Ir(miF)_3$ (green), $Ir(ppy)_3$ (blue) and $Ir(ppyCF_3)_3$ (purple). c.) Current density-voltage-luminance curve for all iridium complexes. d.) EQE versus current density for all iridium complexes. Inset is the molecular structures of materials used in the devices.

The modal power distributions of the PHOLEDs were calculated based on Green's function analysis, using the Θ values determined by ADPS and FPIM (see SI for details).[39] This analysis, with results in **Figure 7,** allows us to estimate the fraction of the EL emission in the forward direction (air mode) versus waveguided modes in the OLED and in the glass substrate, and surface plasmon modes in the cathode. As shown in **Table 3**, outcoupling efficiencies (air mode) are consistent with the

degree of dopant alignment from the ADPS and FPIM measurements: outcoupling is highest for $Ir(mip)_3$ with 32.8% of the light forward scattered, compared to 24.6 % for $Ir(ppy)_3$. Simulated EQEs were obtained by multiplying Φ_{PL} by the calculated outcoupling efficiency of each dopant (**Table 3**), showing a close correspondence between the measured and predicted EQE values for a given value of Θ. The discrepancy between experimental and simulated EQEs is the largest when $Ir(miF)_3$ is the dopant. This could be due to a small difference in the Θ value for $Ir(miF)_3$ in the mixed host as compared to Θ in mCBP (0.8 D) and TCTA (0.1 D) hosts (Table 2), given that the magnitude of PDM of $Ir(miF)_3$ (12.7 D) is higher than those of $Ir(mi)_3$ (6.9 D) and $Ir(mip)_3$ (6.7 D).

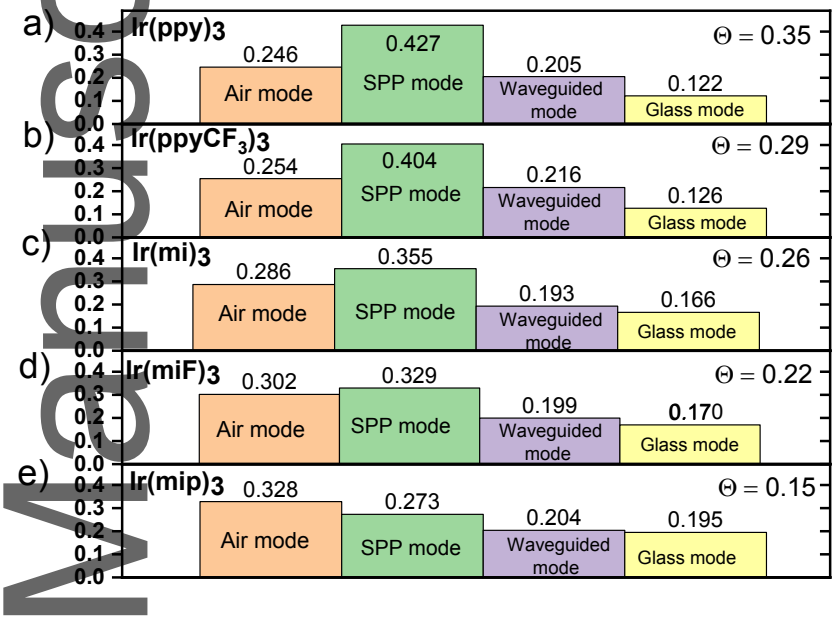

Figure 7. Simulated outcoupling efficiencies (Air mode) and the probability of light being dissipated to other modes (Surface Plasmon Polarization mode, waveguided mode and glass mode) for $Ir(ppy)_3$ (a), $Ir(ppyCF_3)_3$ (b), $Ir(mi)_3$ (c), $Ir(miF)_3$ (d) and $Ir(mip)_3$ (e) in TCTA:26DCzPPy mixed host, with the device architecture used for the devices represented in Figure 6.

The turn-on voltage (V_T = voltage at 0.1 cd/m^2) for OLEDs using the non-fluorinated dopants range from 2.5-2.9 V, whereas the V_T of OLEDs using $Ir(miF)_3$ and $Ir(ppyCF_3)_3$ are 3.9 V and 4.5V, respectively (**Figure 6c**). The larger V_T for the devices with CF_3 substituted dopants is attributed to a large interfacial dipole from spontaneous ordering of dopant PDMs at the EML/ETL interface.[40] It has been reported that a polarized interface can strongly affect charge transport and injection.[41] The PDMs estimated from DFT calculations for the non-fluorinated dopants are 6.4-6.9 D, whereas those of the CF_3 substituted derivatives are 12.7 and 16.3 D for $Ir(miF)_3$ and $Ir(ppyCF_3)_3$, respectively (**Table 1**). In the emitters studied here, the PDM coincides with the C_3 axis of the molecule (Figure S18). Thus, the increase in V_T suggests that $Ir(miF)_3$ and $Ir(ppyCF_3)_3$ are aligned with the CF_3 groups oriented toward the vacuum interface during the deposition. This ordering polarizes the HTL/EML interface to hinder injection of holes into the EML, which shifts the J-V curve to higher voltages, as observed.

Conclusion

The relationship between the shapes of three homoleptic *tris*-cyclometalated Ir complexes and their degree of alignment when doped into vacuum deposited thin films was investigated using angle dependent photoluminescence spectroscopy and Fourier-plane imaging microscopy. Molecules with oblate spheroidal shapes show the highest degree of in-plane alignment, with the long axis of the electronic density ellipsoid showing a net parallel alignment relative to the substrate. The driving force for this process is likely due to enhanced van der Waals interactions of the higher surface polar area "face" over the equatorial "edge" of the ellipsoid. Thus, molecules with spherical, or near spherical shapes are expected to show no preferred orientation in the vacuum deposited films, as observed for complexes with a low aspect ratio such as $Ir(ppy)_3$.

Addition of trifluoromethyl substituents onto one polar face of the *tris*-cyclometalated Ir complexes demonstrate the role of chemical asymmetry in the alignment of molecules. The CF_3 groups in $Ir(miF)_3$ and $Ir(ppyCF_3)_3$ make their shapes less oblate, which should promote isotropic orientation in doped thin films. This is not the case, however, as films doped with the fluorinated derivatives have anisotropy factors that are lower than those using the parent complexes. The fluorinated "patch" on the surface of the complexes has a lower affinity for the surface of the host matrix owing to a decrease in van der Waals interactions. The asymmetry in molecular attraction is expected to favor an orientation of the dopant with the fluorinated face of the complex directed away from the surface toward the vacuum during deposition.

This work provides two approaches to achieve net alignment of *tris*-cyclometalated Ir complexes in vacuum deposited films. Altering the molecular shape to approximate an oblate spheroid or adding functional groups to one face of the molecule can lead to a net horizontal alignment of the transition dipole moments in doped films. While the oblate shape may drive the complex toward a parallel arrangement relative to the substrate, the principal axis of the molecule can be directed either toward or away from the substrate. The addition of trifluoromethyl substituents to one face of the molecule will not only promote net alignment relative to the substrate but can also orient of the principal axis of the complex to be directed either toward or away from the substrate, depending on the site of substitution. Moreover, these two effects, when acting in concert, can lead to further improvement in the degree of horizontal alignment, and hence lead to a higher outcoupling efficiency when used in OLEDs.

Supporting Information

The syntheses and characterizations of all $Ir(C^N)_3$ compounds are given in Scheme1, Figure S1-17 and Table S1-2 (S4-17). Details of DFT calculations, computational modeling and calculation of aspect ratios are provided in S20-24. Information on OLED device simulation and fabrication is presented in S27-29. ADPS and FPIM results for all $Ir(C^N)_3$ complexes doped into hosts films are given in S26-28.

Acknowledgements

This work was supported by the Universal Display Corporation. SRF also acknowledges support from the Air Force Office of Scientific Research, Grant No. 17RT0908. The authors would like to thank Dr. Muazzam Idris for help with the synthesis of $Ir(mip)_3$.

References

[1] G. Hong, X. M. Gan, C. Leonhardt, Z. Zhang, J. Seibert, J. M. Busch, S. Brase, Adv. Mater. **2021**, *33*.

[2] W. Brütting, J. Frischeisen, T. D. Schmidt, B. J. Scholz, C. Mayr, Phy. Status Solidi A **2013**, *210*, 44.

[3] Y. Watanabe, H. Sasabe, J. Kido, Bull. Chem. Soc. Jpn. **2019**, *92*, 716.

[4] N. C. Greenham, R. H. Friend, D. D. C. Bradley, Adv. Mater. **1994**, *6*, 491; L. H. Smith, J. A. E. Wasey, I. D. W. Samuel, W. L. Barnes, Adv. Funct. Mater. **2005**, *15*, 1839.

[5] M. C. Gather, S. Reineke, Journal of Photonics for Energy **2015**, *5*, 20; A. Salehi, X. Y. Fu, D. H. Shin, F. So, Adv. Funct. Mater. **2019**, *29*.

[6] C. F. Madigan, M. H. Lu, J. C. Sturm, Appl. Phys. Lett. **2000**, *76*, 1650; S. Möller, S. R. Forrest, J. Appl. Phys. **2002**, *91*, 3324; X. Huang, Y. Qu, D. Fan, J. Kim, S. R. Forrest, Org. Electron. **2019**, *69*, 297.

[7] Y. Qu, J. Kim, C. Coburn, S. R. Forrest, ACS Photonics **2018**, *5*, 2453.

[8] T. Yamasaki, K. Sumioka, T. Tsutsui, Appl. Phys. Lett. **2000**, *76*, 1243; P. Y. Ang, P.-A. Will, S. Lenk, A. Fischer, S. Reineke, Sci. Rep. **2019**, *9*, 18601.

[9] X. Huang, Y. Qu, D. Fan, J. Kim, S. Forrest, Organic Electronics **2019**, *69*, 297; B. Riedel, I. Kaiser, J. Hauss, U. Lemmer, M. Gerken, Opt. Express **2010**, *18*, A631.

[10] M. Flämmich, J. Frischeisen, D. S. Setz, D. Michaelis, B. C. Krummacher, T. D. Schmidt, W. Brütting, N. Danz, Org. Electron. **2011**, *12*, 1663; J. Frischeisen, D. Yokoyama, A. Endo, C. Adachi, W. Brutting, Org. Electron. **2011**, *12*, 809; T. D. Schmidt, D. S. Setz, M. Flammich, J. Frischeisen, D. Michaelis, B. C. Krummacher, N. Danz, W. Brutting, Appl. Phys. Lett. **2011**, *99*; K.-H. Kim, J.-J. Kim, Adv. Mater. **2018**, *30*, 1705600.

[11] K.-H. Kim, S. Lee, C.-K. Moon, S.-Y. Kim, Y.-S. Park, J.-H. Lee, J. Woo Lee, J. Huh, Y. You, J.-J. Kim, Nat. Commun. **2014**, *5*, 4769.

[12] T. D. Schmidt, T. Lampe, D. Sylvinson M. R, P. I. Djurovich, M. E. Thompson, W. Brütting, Phys. Rev. Appl. **2017**, *8*, 037001.

[13] J. S. Kim, D. Jeong, H. J. Bae, Y. Jung, S. Nam, J. W. Kim, S. G. Ihn, J. Kim, W. J. Son, H. Choi, S. Kim, Advanced Optical Materials **2020**, *8*, 2001103.

[14] J. Frischeisen, D. Yokoyama, C. Adachi, W. Brütting, Appl. Phys. Lett. **2010**, *96*, 073302.

[15] C. K. Moon, K. H. Kim, J. J. Kim, Nat. Commun. **2017**, *8*.

[16] T. Lee, B. Caron, M. Stroet, D. M. Huang, P. L. Burn, A. E. Mark, Nano Lett. **2017**, *17*, 6464.

[17] A. Graf, P. Liehm, C. Murawski, S. Hofmann, K. Leo, M. C. Gather, J. Mater. Chem. C **2014**, *2*, 10298.

[18] M. D. Ediger, J. de Pablo, L. Yu, Acc. Chem. Res. **2019**, *52*, 407.

[19] D. Yokoyama, Journal of Materials Chemistry **2011**, *21*, 19187.

[20] J. S. Huh, K. H. Kim, C. K. Moon, J. J. Kim, Org. Electron. **2017**, *45*, 279.

[21] J. Kim, T. Batagoda, J. Lee, D. Sylvinson, K. Ding, P. J. G. Saris, U. Kaipa, I. W. H. Oswald, M. A. Omary, M. E. Thompson, S. R. Forrest, Adv. Mater. **2019**, *31*, 1900921.

[22] M. J. Jurow, C. Mayr, T. D. Schmidt, T. Lampe, P. I. Djurovich, W. Brütting, M. E. Thompson, Nat. Mater. **2016**, *15*, 85.

[23] M. Schmid, K. Harms, C. Degitz, T. Morgenstern, A. Hofmann, P. Friederich, H. H. Johannes, W. Wenzel, W. Kowalsky, W. Brutting, Acs Applied Materials & Interfaces **2020**, *12*, 51709.

[24] K. Udagawa, H. Sasabe, C. Cai, J. Kido, Adv. Mater. **2014**, *26*, 5062.

[25] C. K. Moon, S. Y. Kim, J. H. Lee, J. J. Kim, Opt. Express **2015**, *23*, A279.

[26] J. Kim, H. Zhao, S. Hou, M. Khatoniar, V. Menon, S. R. Forrest, Physical Review Applied **2020**, *14*.

[27] M. Nonoyama, Bull. Chem. Soc. Jpn. **1974**, *47*, 767.

[28] J. Y. Zhuang, W. F. Li, W. C. Wu, M. S. Song, W. M. Su, M. Zhou, Z. Cui, New J. Chem. **2015**, *39*, 246.

[29] M. E. Thompson, P. E. Djurovich, S. Barlow, S. Marder, in *Comprehensive Organometallic Chemistry III*, Vol. 12 (Ed: D. O'Hare), Elsevier Ltd., Oxford, UK 2007, 102.

[30] E. van Lenthe, E. J. Baerends, J. G. Snijders, J.Chem.Phys. **1994**, *101*, 9783; E. vanLenthe, J. G. Snijders, E. J. Baerends, J. Chem. Phys. **1996**, *105*, 6505; E. v. Lenthe, E. J. Baerends, J. G. Snijders, J.Chem.Phys. **1993**, *99*, 4597; M. Babazadeh, P. L. Burn, D. M. Huang, PCCP **2019**, *21*, 9740.

[31] J. Sworakowski, Synth. Met. **2018**, *235*, 125.

[32] K.-H. Kim, E. S. Ahn, J.-S. Huh, Y.-H. Kim, J.-J. Kim, Chem. Mater. **2016**, *28*, 7505.

[33] K.-H. Kim, C.-K. Moon, J.-H. Lee, S.-Y. Kim, J.-J. Kim, Adv. Mater. **2014**, *26*, 3844.

[34] T. Lampe, T. D. Schmidt, M. J. Jurow, P. I. Djurovich, M. E. Thompson, W. Brütting, Chem. Mater. **2016**, *28*, 712.

[35] E. R. Vorpagel, J. G. Lavin, Carbon **1992**, *30*, 1033.

[36] C.-K. Moon, K.-H. Kim, J. W. Lee, J.-J. Kim, Chem. Mater. **2015**, *27*, 2767.

[37] M. Giese, M. Albrecht, K. Rissanen, Chem. Commun. (Camb.) **2016**, *52*, 1778; J. D. Mottishaw, H. Sun, J. Phys. Chem. A **2013**, *117*, 7970.

[38] K. Udagawa, H. Sasabe, F. Igarashi, J. Kido, Adv. Opt. Mater. **2016**, *4*, 86.

[39] R. R. Chance, A. Prock, R. Silbey, J.Chem.Phys. **1974**, *60*, 2744; K. Celebi, T. D. Heidel, M. A. Baldo, Opt. Express **2007**, *15*, 1762.

[40] Y. Noguchi, H. Lim, T. Isoshima, E. Ito, M. Hara, W. Won Chin, J. Wook Han, H. Kinjo, Y. Ozawa, Y. Nakayama, H. Ishii, Appl. Phys. Lett. **2013**, *102*; K. Osada, K. Goushi, H. Kaji, C. Adachi, H. Ishii, Y. Noguchi, Org. Electron. **2018**, *58*, 313.

[41] L. Jäger, T. D. Schmidt, W. Brütting, AIP Adv. **2016**, *6*, 095220; Y. Noguchi, W. Brütting, H. Ishii, Jap. J. Appl. Phys. **2019**, *58*, SF0801; J. S. Bangsund, J. R. Van Sambeek, N. M. Concannon, R. J. Holmes, Sci Adv **2020**, *6*, eabb2659; Y. Noguchi, W. Brütting, H. Ishii, Jpn. J. Appl. Phys. **2019**, *58*.

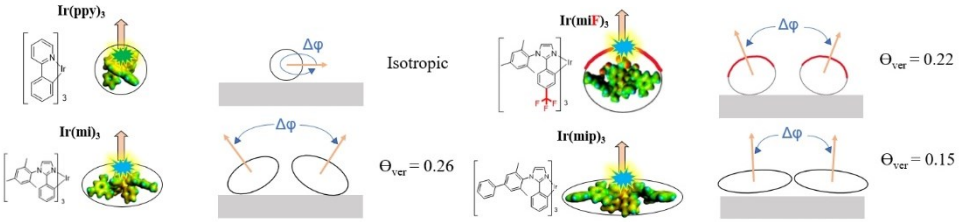

Dopant alignment in doped, vacuum deposited films can be promoted by molecular asymmetry and/or asymmetry in the dopant's electrostatic surface potential.